Research Article

Phytochemical Analysis

Received: 4 November 2012, Revised: 28 January 2013, Accepted: 30 January 2013 Published online in Wiley Online Library: 17 April 2013

(wileyonlinelibrary.com) DOI 10.1002/pca.2431

10991565, 2013, 6, Downloaded from https://analyticalsciencejournals.onlinelibrary.wiley.com/doi/10.1002/pca.2431 by INASP - KENYA Maseno University, Wiley Online Library on [05/11/2022]. See the Terms and Conditions (https://onlinelibrary.wiley.com/terms-and-conditions) on Wiley Online Library for rules of use; OA articles are governed by the applicable Creative Commons License

A Novel Approach in Herbal Quality Control Using Hyperspectral Imaging: Discriminating Between *Sceletium tortuosum* and *Sceletium crassicaule*

Emmanuel Amukohe Shikanga,[a] Alvaro M. Viljoen,[b]* Ilze Vermaak[b] and Sandra Combrinck[a]

ABSTRACT:

Introduction – *Sceletium tortuosum* is the most sought after species of the genus *Sceletium* and is commonly included in commercial products for the treatment of psychiatric conditions and neurodegenerative diseases. However, this species exhibits several morphological and phytochemical similarities to *S. crassicaule*.

Objectives – The aim of this investigation was to use ultrahigh-performance liquid chromatography (UPLC) and hyperspectral imaging, in combination with chemometrics, to distinguish between *S. tortuosum* and *S. crassicaule*, and to accurately predict the identity of specimens of both species.

Methods – Chromatographic profiles of *S. tortuosum* and *S. crassicaule* specimens were obtained using UPLC with photodiode array detection. A SisuChema near infrared hyperspectral imaging camera was used for acquiring images of the specimens and the data was processed using chemometric computations.

Results – Chromatographic data for the specimens revealed that both species produce the psychoactive alkaloids that are used as quality control biomarkers. Principal component analysis of the hyperspectral image of reference specimens for the two species yielded two distinct clusters, the one representing *S. tortuosum* and the other representing *S. crassicaule*. A partial least squares discriminant analysis model correctly predicted the identity of an external dataset consisting of *S. tortuosum* or *S. crassicaule* samples with high accuracy (>94%).

Conclusions – A combination of hyperspectral imaging and chemometrics offers several advantages over conventional chromatographic profiling when used to distinguish *S. tortuosum* from *S. crassicaule*. In addition, the constructed chemometric model can reliably predict the identity of samples of both species from an external dataset. **Copyright © 2013 John Wiley & Sons, Ltd.**

Keywords: Chemometrics; hyperspectral imaging; PCA; PLS–DA; *Sceletium crassicaule*; *Sceletium tortuosum*

Introduction

Sceletium tortuosum (L.) N.E.Br (Mesembryanthemaceae), a succulent sub-shrub endemic to South Africa, is the most popular and commonly used species of the genus *Sceletium* (van Wyk and Gericke, 2003). This species has received a great deal of interest due to its potential as an adaptogen for relieving stress in healthy people, and for treating a broad range of psychological, psychiatric and inflammatory conditions (Gericke, 2001; Gericke and Viljoen, 2008). Scientific investigations have proved that *S. tortuosum* produces mesembrine-type alkaloids (mesembrenol, mesembranol, mesembrenone and mesembrine), which are responsible for the psychoactive properties of the plant (Smith *et al*., 1996). The ability of these alkaloids to inhibit serotonin re-uptake and the PDE-4 enzyme, are thought to play a role in the treatment of a variety of disorders related to the central nervous system (Gericke and Viljoen, 2008; Harvey *et al*., 2011). A demand for *S. tortuosum* products has stimulated commercial interest in these products (www.Sceletium.org. 2007). Large plantations of *S. tortuosum* have been established in the three Cape provinces of South Africa, as well as in Namibia. A range of product formulations derived from this species, including extracts, capsules, tablets, sprays, teas and tinctures, are traded both locally and abroad.

Owing to the large number of commercial products on the market, quality control methods for authentication of *S. tortuosum* raw materials and products are vital. Quality assurance systems are aimed at providing the consumer with high quality, effective and safe products, while ensuring profitability for the producers (Tadmor *et al*., 2002). *Sceletium tortuosum* is mainly distinguished from other *Sceletium* species by comparing the vegetative, flower, fruit and seed characteristics. However, this species shares various morphological similarities, such as

* Correspondence to: A. Viljoen, Department of Pharmaceutical Sciences, Tshwane University of Technology, Private Bag X680, Pretoria, 0001, South Africa. E-mail: viljoenam@tut.ac.za

[a] Department of Chemistry, Tshwane University of Technology, Private Bag X680, Pretoria, 0001, South Africa

[b] Department of Pharmaceutical Sciences, Tshwane University of Technology, Private Bag X680, Pretoria, 0001, South Africa

 Copyright © 2013 John Wiley & Sons, Ltd.

leaf shape, size and venation pattern, as well as similar flower and seed colouration, with *Sceletium crassicaule* (Haw.) L.Bolus (Gerbaulet, 1996; Gaffney, 2006). In addition, the two species have a sympatric distribution and both produce the four psychoactive alkaloids.

Analytical methods, including capillary electrophoresis, high-performance thin-layer chromatography (HPTLC), high-performance liquid chromatography (HPLC), ultrahigh-performance liquid chromatography (UPLC) and gas chromatography with mass spectrometry detection (GC–MS) have been developed for phytochemical profiling and quantitative determination of the psychoactive alkaloids in *S. tortuosum* raw materials and products (Smith *et al*., 1998; van Wyk and Gericke, 2003; Patnala and Kanfer, 2009, 2010; Shikanga *et al*., 2012a–c).

Vibrational spectroscopy techniques, including Fourier transform near infrared (FT–NIR) and FT–mid-infrared (FT–MIR) spectroscopy, have been used for quality control of agricultural, pharmaceutical, cosmetic products and herbal medicines (Sinija and Mishra, 2009) as well as for quality assessment of foods, including pepper, grapefruit, pumpkin, carrot and tomato (Schulz and Baranska, 2007). The IR techniques generate spectra that provide information reflecting the chemical composition of a sample. Spectral data are useful for the discrimination of different species, and also for the identification of chemotypes or cultivars within the same species. Advancements in conventional IR spectroscopy have resulted in the development of the hyperspectral imaging (HSI) technique, which is a combination of spectroscopy and digital imaging (Gowen *et al*., 2008). Conventional spectroscopic methods cannot measure the internal constituent gradients within a sample, since spatial information cannot be captured (Gowen *et al*., 2008). This limitation results in discrepancies between measured and predicted compositions.

A hyperspectral image, also referred to as a three-dimensional hypercube, is a combination of spectral information, across a wide range of spectral bands, and spatial information, gathered over a defined region of a sample (Furukawa *et al*., 2007; Gowen *et al*., 2008). A hypercube consists of two spatial dimensions (*X* and *Y*) and one wavelength (*Z*) coordinate (Gowen *et al*., 2008). This information is simultaneously collected in two dimensions, whereafter a three-dimensional image is created by sequential stacking of the two-dimensional slices. A hypercube is made up of hundreds of wavebands, each representing a spatial position (pixel area) within the sample. This process yields information-dense datasets, which require a multidisciplinary processing approach involving advanced image processing and multivariate statistical techniques, such as chemometrics (Furukawa *et al*., 2007). Owing to the abundance of information contained in a hyperspectral image, this technique has numerous practical applications in a variety of fields (Gowen *et al*., 2008).

This study was initiated to compare the alkaloid UPLC profiles of *S. tortuosum* and *S. crassicaule*, in order to distinguish these morphologically similar species. The application of hyperspectral imaging as a novel tool to differentiate the species was also explored.

Materials and methods

Reagents and materials

High-purity solvents purchased from Merck (Darmstadt, Germany) were used for alkaloid extraction and later analysis of the extracts using UHPLC. Methanol, ammonia (25% w/w), sulphuric acid (98% w/w) and dichloromethane were AR grade, while acetonitrile for UPLC analysis was HPLC grade. The reference standards (mesembrine, mesembrenol, mesembranol and mesembrenone), were isolated from *S. tortuosum* using high speed countercurrent chromatography (Shikanga *et al*., 2011). These compounds were characterised by ^{1}H- and ^{13}C- (one and two-dimensional) nuclear magnetic resonance spectroscopy, GC–MS and by comparison of the data with those reported in the literature.

Plant material

Aerial parts of wild *S. tortuosum* and *S. crassicaule* plants were collected from various localities in the Cape region of South Africa in October 2009. Voucher specimens were deposited at the Department of Pharmaceutical Sciences at Tshwane University of Technology. Samples with voucher specimen numbers SCT007, SCT035, SCT064, SCT128 and SCT138, each representing one of five identified chemotypes of *S. tortuosum* (Shikanga *et al*., 2012c), and *S. crassicaule* specimens SCC001, SCC003, SCC004, SCC009 and SCC011, were selected as reference samples for the analysis. The samples with voucher specimen numbers SCT028, 081 and 134 (*S. tortuosum*) and SCC005, 007 and 010 (*S. crassicaule*) were selected for use as test samples.

Sample preparation

The aerial plant parts were dried in an oven (Labotec Ltd, Midrand, South Africa) at 30°C for 2 weeks prior to extraction. Dry plant material was pulverised using a Retsch® MM 400 ball mill (frequency 30 Hz, time 2 min) from Monitoring and Control (Pty) Ltd (Haans, Germany) and sieved using a 500 μm mesh sieve (Endcotts Filters Ltd, London).

Ultrahigh-performance liquid chromatography

Chromatographic profiling of the alkaloid extracts of *S. tortuosum* and *S. crassicaule* samples was performed using a validated UPLC method, previously developed in our laboratory (Shikanga *et al*., 2012b). The UPLC system used comprised a Waters Acquity UPLC sample manager (Waters, Ireland), a binary solvent manager and a photo diode array detector (210 – 400 nm). Separation was achieved using a Waters Acquity reversed phase UPLC BEH C_{18} column (2.1 × 150 mm, 1.7 μm particle size), fitted with a Van Guard pre-column (2.1 × 5 mm, 1.7 μm), both supplied by Waters. An injection volume of 1 μL was applied and the sample and column temperatures were adjusted to 25 and 30° C, respectively. The mobile phase, at a flow rate of 0.3 mL/min, consisted of (A) 0.1% aqueous ammonia and (B) acetonitrile. Gradient elution was employed, starting with 80% A and 20% B, changing to 40% B in 2 min, then changing to 50% B in 2 min and held constant for 3 min, with a post-run time of 1 min.

Hyperspectral imaging

Hyperspectral imaging analysis was conducted using the SisuChema shortwave infrared (SWIR) pushbroom hyperspectral spectrophotometer (Specim Spectral Imaging Ltd, Oulu, Finland), coupled to a two-dimensional array mercury–cadmium–telluride detector. The images were acquired using a macrolens (10 mm) camera with 100 mm × 100 mm field of view. The illumination system (light source) consisted of quartz

Copyright © 2013 John Wiley & Sons, Ltd.

10991565, 2013, 6, Downloaded from https://analyticalsciencejournals.onlinelibrary.wiley.com/doi/10.1002/pca.2431 by INASP - KENYA Maseno University, Wiley Online Library on [05/11/2022]. See the Terms and Conditions (https://onlinelibrary.wiley.com/terms-and-conditions) on Wiley Online Library for rules of use; OA articles are governed by the applicable Creative Commons License

halogen lamps producing dual linear light, covering a spectrum range of 920–2514 nm. Data were obtained with a resolution of 10 nm, at a rate of 6.3 nm spectral sampling per pixel and a frequency of 100 Hz. The exposure time was 3.0 μs. Chemadaq version 3.62.183.19 software (Specim Spectral Imaging Ltd, Oulu, Finland) was used to acquire the data.

Five powdered samples of each species (reference samples of *S. tortuosum* and *S. crassicaule*), were placed on a mobile plane carriage that moves along a horizontal axis beneath the stationary camera. The full spectrum of each individual point of the sample area was measured by line-scanning across the samples by the camera. A hyperspectral reference image (hypercube) was acquired in diffuse reflectance mode. An image, consisting of three specimens of each species constituting the external dataset, was also acquired using identical settings.

Prior to chemometric analysis, spectral unfolding was conducted by appending the two spatial dimensions. This is achieved by rearranging the three-dimensional hypercube into a two-dimensional matrix (Gowen *et al*., 2008). Evince chemometric software version 2.5.0 from Umbio AB (Umea, Sweden) was used to process the spectral data by converting raw images, which had been corrected for white and dark references to pseudo-absorbance (A/D converter counts) data.

A mean centred principal component analysis (PCA) model was constructed, in which the scores image and the scores plot were used interactively to eliminate the background and edge effects (Manley *et al*., 2011). After eliminating the background from the hyperspectral image, the original spectra of the reference samples were then pre-treated by applying various spectral pre-processing methods. The methods applied were standard normal variate (SNV) correction, first and second derivative, as well as multiplicative scatter (MSC) correction. Standard normal variate correction was then selected for spectral pre-treatment, after which, a PCA plot was constructed to indicate the clustering patterns of the different samples in the reference image. A partial least-squares discriminate analysis (PLS–DA) model was then constructed from the PCA model to classify the samples in the reference image. The same model was further applied for the prediction of class membership of the samples constituting the external dataset.

Results and discussion

Reversed phase UPLC analysis

Compounds in the extracts were identified based on retention time and by spiking with reference standards. Representative chromatograms of three *S. tortuosum* and three *S. crassicaule* specimens are illustrated in Figs 1 and 2. All four mesembrine-type alkaloids were identified in the selected specimens, with the exception of sample SC035 (chromatogram not shown), which represented a chemotype of *S. tortuosum* that is devoid of the psychoactive alkaloids. From the results, it can be observed that the alkaloid profiles of specimens of both *S. tortuosum* and *S. crassicaule* were variable. Mesembrine, mesembrenone and mesembrenol were the main constituents of *S. tortuosum* samples SCT064, SCT128 and SCT135, respectively. However, in the *S. crassicaule* specimens, mesembrine was the most abundant alkaloid in SCC003 and SCC004, while mesembrenol was the major constituent in SCC009. It should, however, be noted that *S. tortuosum* samples were collected from different localities, while *S. crassicaule* samples were collected from one locality as it has a more limited distribution.

Our previous investigation of the alkaloid profiles of *S. tortuosum* using GC–MS indicated both intra- and interpopulation variations of the mesembrine-type alkaloids (Shikanga *et al*., 2012b, 2012c). Although chromatographic methods are widely accepted for fingerprinting or profiling of secondary metabolites in plants (Hu *et al*., 2006), the UPLC method was not adequate for distinguishing *S. tortuosum* from *S. crassicaule* specimens. This result can be attributed to the variability of the alkaloid profiles of the two species. However, the method was ideal for quantitative determination of the psychoactive alkaloids in *S. tortuosum* (Shikanga *et al*., 2012c).

Analysis of *S. tortuosum* and *S. crassicaule* specimens using hyperspectral imaging

Principal component analysis was employed to compress and simplify the multi-dimensional hyperspectral image information obtained from the *S. tortuosum* and *S. crassicaule* reference samples. This method is an unsupervised classification method that does not require prior information on the dataset and is used mainly as an exploratory tool to extract important features from a dataset (clustering patterns) (Gowen *et al*., 2008). The PCA scores image and scores plot, which were interactively used to remove unwanted pixels comprising background and edge effects from the hyperspectral image of the reference samples, are depicted in Figs 3 and 4, respectively. The pixel size is 312.5 μm. In the PCA scores image (Fig. 3) it is evident that the central parts of each sample image is more representative of the classes than the outer regions as reflectance intensity decreases towards the edge of the powders (Gowen *et al*., 2008).

Non-chemical biases, such as random noise and light scattering effects, originating from surface inhomogeneities and interferences from external light sources, result in anomalies in the prediction model (Burger and Geladi, 2006). Spectral pre-processing techniques are therefore applied to correct for these anomalies in the data. Standard normal variate correction was found to be the most suitable spectral pre-treatment method, since it ensured maximum separation between the two clusters along the first PC. A three-component PCA model, which explains 91.2% of the total variation in the *X* matrix, was constructed for the reference dataset following SNV pre-treatment. The first PC (t1) explains 73.9% of the variation in the hyperspectral image data as indicated in Fig. 4. The average spectra (920–2514 nm) extracted from the hyperspectral image of *S. tortuosum* and *S. crassicaule* reference samples after SNV pre-treatment, are depicted in Fig. 5A and B, respectively. Each figure represents the pixel spectral signatures obtained for each respective category. A pixel is usually characterised by the full NIR spectrum (920–2514 nm).

The reflectance intensities of *S. tortuosum* spectra were higher than those for *S. crassicaule* for each wavelength investigated. Such variations have been reported to result from surface properties of the sample (Gowen *et al*., 2008). Spectral data are pre-processed prior to analysis, to minimise variations originating from surface properties, while retaining the spectral features of the samples to enable characterisation. The SNV correction method is commonly applied to remove variability in reflectance spectra caused by light scattering (Fearn *et al*., 2009).

Copyright © 2013 John Wiley & Sons, Ltd.

10991565, 2013, 6, Downloaded from https://analyticalsciencejournals.onlinelibrary.wiley.com/doi/10.1002/pca.2431 by INASP - KENYA Maseno University, Wiley Online Library on [05/11/2022]. See the Terms and Conditions (https://onlinelibrary.wiley.com/terms-and-conditions) on Wiley Online Library for rules of use; OA articles are governed by the applicable Creative Commons License

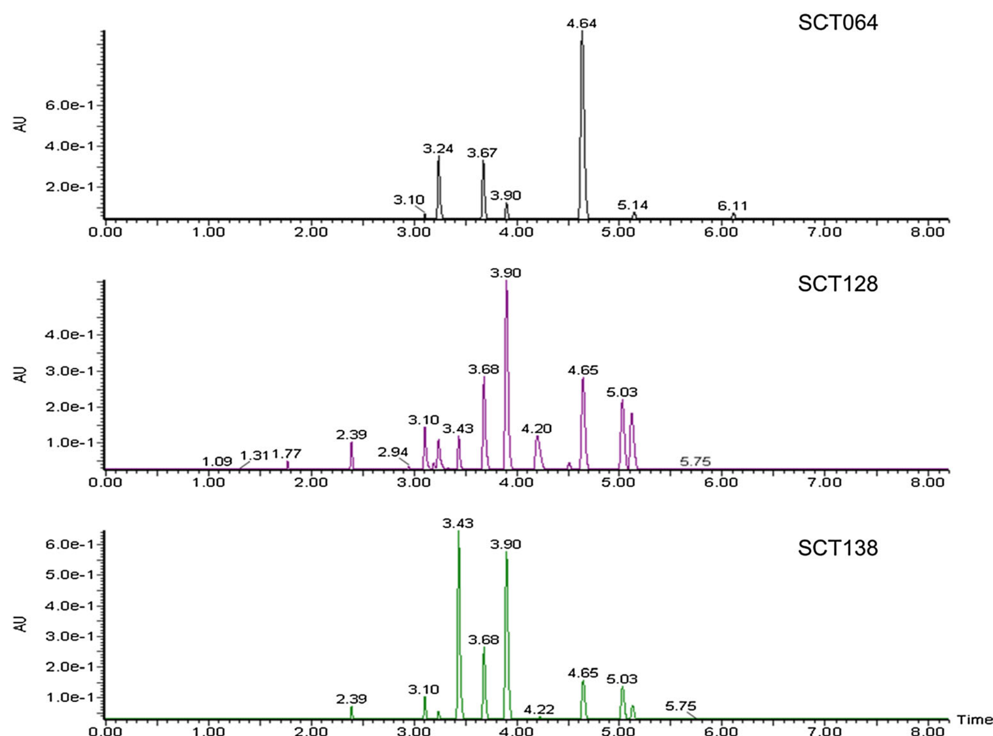

Figure 1. Ultrahigh-performance liquid chromatograms indicating the highly variable alkaloid profiles of *Sceletium tortuosum* specimens, each representing a different chemotype. Chemotypes: SCT064 (mesembrine-rich), SCT128 (mesembrenone-rich), SCT138 (intermediate). Alkaloids: mesembrenol (3.43 min), mesembranol (3.67 min), mesembrenone (3.90 min), mesembrine (4.64 min).

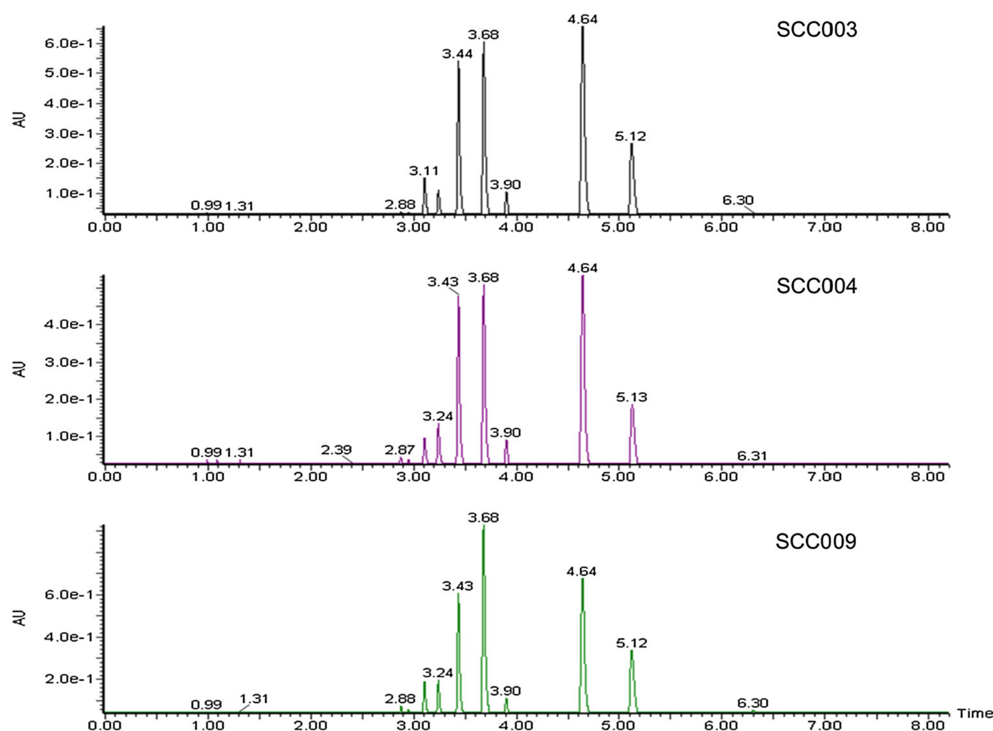

Figure 2. Ultrahigh-performance liquid chromatograms indicating the alkaloid profiles of *Sceletium crassicaule* specimens from Infanta. Alkaloids: mesembrenol (3.43 min), mesembranol (3.67 min), mesembrenone (3.90 min), mesembrine (4.64 min).

In HSI, a PCA model is used to identify regions with similar spectral characteristics, hence providing information on the physiochemical properties of the sample. The use of chemometric data analysis made it possible to distinguish *S. tortuosum* from *S. crassicaule* samples. These results reflect the power of the HSI system to distinguish between *S. tortuosum* and *S. crassicaule*.

Copyright © 2013 John Wiley & Sons, Ltd.

10991565, 2013, 6, Downloaded from https://analyticalsciencejournals.onlinelibrary.wiley.com/doi/10.1002/pca.2431 by INASP - KENYA Maseno University, Wiley Online Library on [05/11/2022]. See the Terms and Conditions (https://onlinelibrary.wiley.com/terms-and-conditions) on Wiley Online Library for rules of use; OA articles are governed by the applicable Creative Commons License

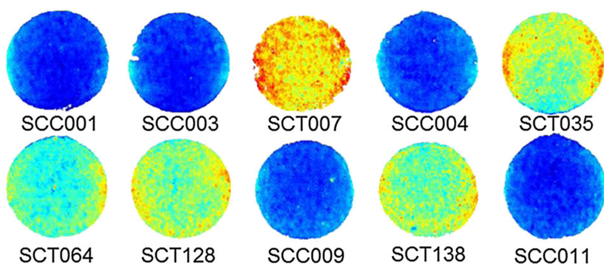

Figure 3. Principal component analysis scores image of *S. tortuosum* (SCT007, 035, 064, 128 and 138) and *S. crassicaule* (SCC001, 003, 004, 009 and 011) specimens.

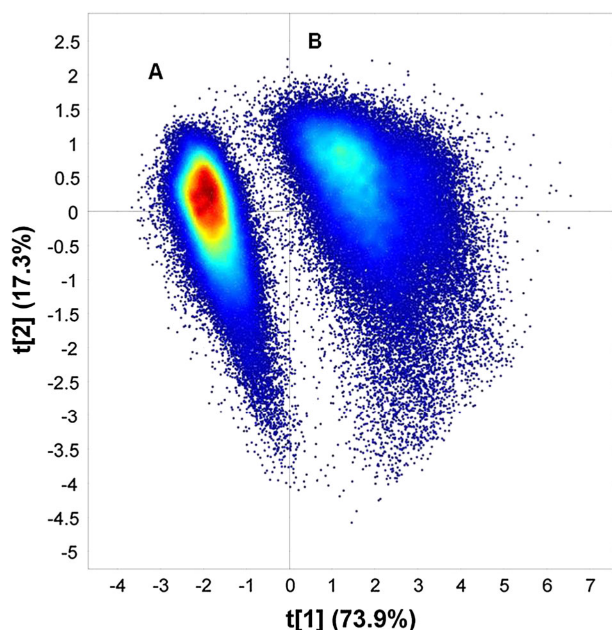

Figure 4. Principal component analysis scores plot indicating the clustering patterns of *S. crassicaule* (A) and *S. tortuosum* (B) specimens.

Prediction of an external dataset using NIR–HSI

A PLS–DA model that is characterised by three PCs, in which 84.3% of the total variation in the *X* matrix along the first PC is explained, was constructed for prediction of external datasets (test set). This classification method is a supervised technique, which requires prior knowledge of the data and is primarily used for prediction of external datasets or for discriminant analysis (Gowen *et al*., 2008). Using this model, test samples in an external dataset consisting of *S. tortuosum* (SCT028, 081, 134) and *S. crassicaule* (SCC005, 007, 010), were correctly identified as illustrated in Fig. 6. The percentage prediction obtained for the test set is determined by the number of correctly predicted pixels. For the *S. tortuosum* dataset consisting of 63580 pixels, as many as 60941 pixels were correctly predicted, whereas out of 63774 pixels of *S. crassicaule*, a total of 61920 were correctly classified. In summary, 95.85% of the pixels from the *S. tortuosum* dataset were correctly predicted, while only 1.59% pixels were incorrectly predicted as *S. crassicaule* and 2.55% pixels remained unclassified. Subsequently, from the *S. crassicaule* dataset, 97.09% of the pixels were correctly predicted, with a mere 0.94% incorrectly predicted as *S. tortuosum*, and the remaining 1.96% not classified. Non-classified pixels typically originate from shading errors or illumination and edge effects. The high level of

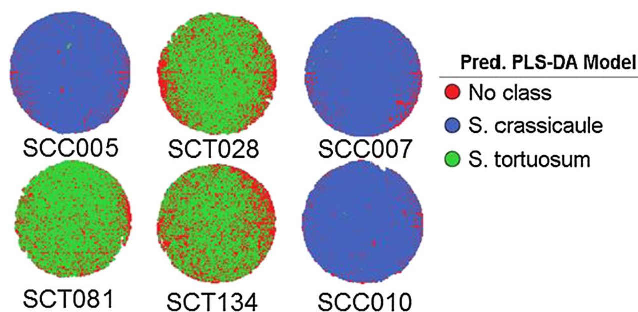

Figure 6. Predicted hyperspectral imaging data obtained from the external dataset of *S. tortuosum* (SCT) and *S. crassicaule* (SCC) test samples.

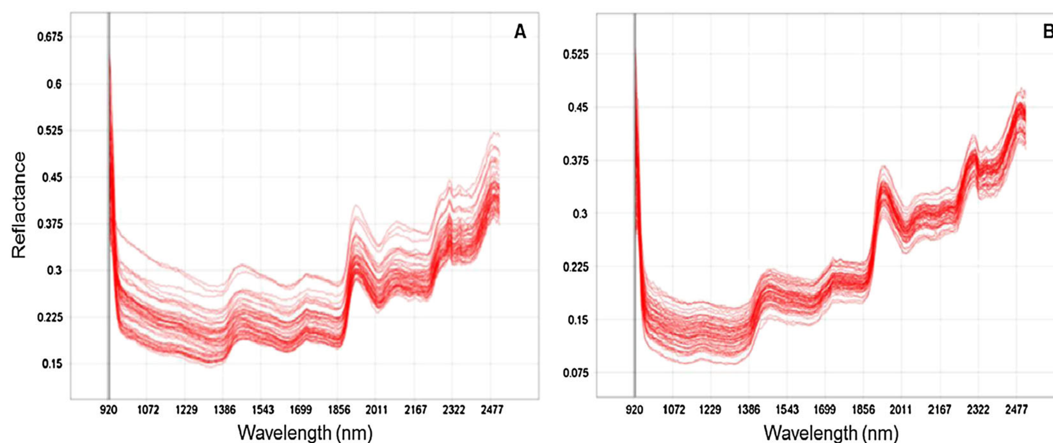

Figure 5. Reflectance spectra for the reference samples of (A) *S. tortuosum* and (B) *S. crassicaule* in the NIR field (920–2514 nm) following SNV pre-treatment.

10991565, 2013, 6, Downloaded from https://analyticalsciencejournals.onlinelibrary.wiley.com/doi/10.1002/pca.2431 by INASP - KENYA Maseno University, Wiley Online Library on [05/11/2022]. See the Terms and Conditions (https://onlinelibrary.wiley.com/terms-and-conditions) on Wiley Online Library for rules of use; OA articles are governed by the applicable Creative Commons License

Copyright © 2013 John Wiley & Sons, Ltd.

prediction of the model is an indication that it is ideal for classification of *S. tortuosum* specimens, regardless of the chemotype selected.

Hyperspectral imaging is increasingly applied for on-line monitoring in food processing to detect differences in chemical composition, colour, or moisture content, as well as for recognising shapes, patterns, defects, contaminants and spatial distributions of other relevant features (Yang *et al*., 2012). By collecting the spectrum for each individual point of the sample by planar scanning, the NIR–HSI instrument can be used to monitor the quality of an entire product line as it passes. In this way, the contaminated or unwanted sample can be easily detected and removed. The short wavelength (SWIR) region, which captures important spectral information from 900 to 2500 nm, is particularly powerful for differentiating components of food products, medicines and botanical substances (Gowen *et al*., 2008).

Although UPLC is an ideal method for quantitative determination of psychoactive alkaloids in *Sceletium* species, the UPLC fingerprints of *S. tortuosum* and *S. crassicaule* specimens could not be used to distinguish the two species. However, NIR–HSI combined with chemometrics proved to be a reliable tool for differentiation of *S. tortuosum* and *S. crassicaule* specimens. The application of SNV data correction was found to be a suitable pre-treatment for the HSI spectral data. The PLS–DA model obtained can be used to accurately classify a sample as *S. tortuosum* or *S. crassicaule*. This method is a non-destructive and time-saving technique with potential application for on-line quality monitoring of *S. tortuosum* raw materials. The HSI system is fast and comprises a low heat-load illumination, making it ideal for on-line, non-destructive sample monitoring. This versatile and environmentally friendly technique is mostly used in the absence of organic solvents (Tripathi and Mishra, 2009), and requires few sample preparation steps, since samples can be analysed in various states, including solids, semi-solids, powders, suspensions and liquids (Gowen *et al*., 2008).

Acknowledgements

The authors thank the National Research Foundation (NRF) of South Africa for funding the research.

References

Burger J, Geladi P. 2006. Hyperspectral NIR image regression part II: dataset processing diagnostics. *J Chemom* **20**: 106–119.
Fearn T, Riccioli C, Garrido-Varo A, Guerrero-Ginel JE. 2009. On the geometry of SNV and MSC. *Chemom Intel Lab Systems* **96**(1): 22–26.
Furukawa T, Sato H, Shinzawa H, Noda I, Ochiai S. 2007. Evaluation of homogeneity of binary blends of poly(3-hydroxybutyrate) and poly(L-lactic acid) studied by near infrared chemical imaging. *Anal Sci* **23**(7): 871–876.
Gaffney CD. 2006. A study of Mesembryanthemaceae alkaloids. MSc. dissertation, University of Johannesburg: Johannesburg; 40–50.
Gerbaulet M. 1996. Revision of the genus *Sceletium* N.E.Br. (Aizoaceae). *Bot Jahrb* **118**: 9–24.
Gericke N. 2001. Clinical application of selected South African medicinal plants. *Australian Journal of Medical Herbalism* **13**: 3–17.
Gericke N, Viljoen AM. 2008. Sceletium – a review update. *J Ethnopharmacol* **119**: 653–663.
Gowen AA, O'Donell CP, Taghizadeh M, Cullen PJ, Frias JM, Downey G. 2008. Hyper-spectral imaging combined with principal component analysis for bruise detection on white mushrooms (*Agaricus bisporus*). *J Chemom* **22**: 259–267.
Harvey AL, Young LC, Viljoen AM, Gericke NP. 2011. Pharmacological actions of South African medicinal and functional food plant *Sceletium tortuosum* and its principle alkaloids. *J Ethnopharmacol* **137**: 1124–1129.
Hu LF, Li SP, Cao H, Liu JJ, Gao JL, Yang FQ, Wang YT. 2006. GC–MS fingerprint of *Pogostemon cablin* in China. *J Pharm Biomed Anal* **42**: 200–206.
Manley M, Du Toit G, Geladi P. 2011. Tracking diffusion of conditioning water in single wheat kernels of different hardness by near infrared hyperspectral imaging. *Anal Chim Acta* **686**: 64–75.
Patnala S, Kanfer I. 2009. Investigation of the phytochemical content of *Sceletium tortuosum* following preparation of '*Kougoed*' by fermentation. *J Ethnopharmacol* **121**: 86–91.
Patnala S, Kanfer I. 2010. HPLC analysis of mesembrine-type alkaloids in *Sceletium* plant material used as an African traditional medicine. *J Pharm Pharm Sci* **13**: 558–570.
Schulz H, Baranska M. 2007. Identification and quantification of valuable plant substances by IR and Raman spectroscopy. *Vib Spec* **43**: 13–25.
Shikanga EA, Viljoen A, Combrinck S, Marston A. 2011. Isolation of *Sceletium* alkaloids by high-speed countercurrent chromatography. *Phytochem Lett* **4**: 190–193.
Shikanga EA, Vermaak, I, Viljoen AM. 2012a. An HPTLC-densitometry method for the quantification of pharmacologically active alkaloids in *Sceletium tortuosum* raw material and products. *JPC-J Planar Chrom* **25**(4): 1–7.
Shikanga EA, Viljoen AM, Combrinck S, Marston A, Gericke N. 2012b. The chemotypic variation of *Sceletium tortuosum* alkaloids and commercial product formulations. *Biochem System Ecol* **44**: 364–373.
Shikanga EA, Kamatou GPP, Chen W, Combrinck S, Viljoen AM. 2012c. Validated RP–UPLC and GC–MS methods for the analysis of psychoactive alkaloids in *Sceletium tortuosum*. *S Afri J Bot* **82**: 99–107.
Sinija S, Mishra HN. 2009. FT–NIR for caffeine estimation in instant tea powder and granules. *Food Sci Technol* **42**: 998–1002.
Smith MT, Crouch NR, Gericke N, Hirst M. 1996. Psychoactive constituents of the genus *Sceletium* N.E.Br. and other Mesembryanthemaceae: a review. *J Ethnopharmacol* **50**: 119–130.
Smith MT, Field CR, Crouch NR, Hirst M. 1998. The distribution of mesembrine alkaloids in selected taxa of the Mesembryanthemaceae and their modification in the *Sceletium* derived '*Kougoed*'. *Pharm Biol* **36**: 173–179.
Tadmor Y, Jefthas E, Goliath J, Smith M, Langenhoven P, Acquaye D, Juliani R, Letchamo W, Renaud E, Zimba N, Raskin I, Brown J, Simon EJ. 2002. Quality assurance and quality control for African natural plant products from ground up. In *Trends in New Crops and New Uses*, Janick J, Whipkey A (eds). ASHS Press: Alexandria; 80–85.
Tripathi S, Mishra HN. 2009. A rapid FT–NIR method for estimation of aflatoxin B_1 in red chilli powder. *Food Control* **20**: 840–846.
Van Wyk B-E, Gericke N. 2003. People's Plants. Briza Publications: Pretoria; 172. www.Sceletium.org (accessed 20 January 2011).
Yang Y, Chai R, He Y. 2012. Early detection of rice blast (*Pyricularia*) at seedling stage in Nippon bare rice variety using near-infrared hyper-spectral image. *Afri J Biotech* **11**(26): 6809–6817.

Copyright © 2013 John Wiley & Sons, Ltd.

10991565, 2013, 6, Downloaded from https://analyticalsciencejournals.onlinelibrary.wiley.com/doi/10.1002/pca.2431 by INASP - KENYA Maseno University, Wiley Online Library on [05/11/2022]. See the Terms and Conditions (https://onlinelibrary.wiley.com/terms-and-conditions) on Wiley Online Library for rules of use; OA articles are governed by the applicable Creative Commons License